Wind and wave dataset for Matara, Sri Lanka

Yao Luo[1], Dongxiao Wang[1]*, Tilak Priyadarshana Gamage[2], Fenghua Zhou[1], Charith Madusanka Widanage[1], Taiwei Liu[3]

[1] *State Key Laboratory of Tropical Oceanography, South China Sea Institute of Oceanology, Chinese Academy of Sciences, Guangzhou 510301, China.*

[2] *University of Ruhuna, Matara 810000, Sri Lanka*

[3] *China Harbour Engineering Company Ltd., Beijing 100027, China*

*Corresponding author: Dongxiao Wang (dxwang@scsio.ac.cn)

Abstract

We present the first continuous in situ hydro-meteorology observations from the south of Sri Lanka from a set of instruments deployed firstly in December 2012. The simultaneously record wind and wave data in this region are sparse due to difficulties in deployment. Here the survey, deployment and measurements of wind and wave are described with the aim of giving a future user of the data set as comprehensive information as possible. This study reviewed on-going access to the datasets of this survey project. The archived dataset was examined in detail, including wave data at two locations with water depths of 20 m and 10 m comprising synchronous time-series of wind, ocean astronomical tide, atmospheric pressure and so on. In addition, we use these wave observations to evaluate the ERA-Interim reanalysis product and demonstrate that it represented near-shore waves in this region not very well. The buoy 2 observations showed that the swell is the main parts in all year and the monsoon can markedly adjusted the proportion between swell and wind sea. The data set made publicly available from Science Data Bank (http://www.sciencedb.cn/dataSet/handle/447).

Key words: wave; wind; observations; Indian Ocean; Sri Lanka

Table 1 Dataset Profile

Dataset title	Wind and wave dataset for Matara, Sri Lanka		
Time range	Wave observations: 2013.9–2014.2 and 2013.4–2014.4 Wind and air pressure observations: 2012.12–2014.6 and 2015.12–2016.10		
Geographic scope	Sri Lanka; North Indian Ocean		
Data format	".xlsx" for observed data	Data volume	5.63 Mb for the 30-min or 10-min observations of wind and waves
Data service system	http://www.sciencedb.cn/dataSet/handle/447 DOI: 10.11922/sciencedb.447		

1 Background & Summary

Ocean observational data are difficult to obtain, but are needed for model validation and data assimilation. Specifically, wind and wave observational data are of great importance for the study of ocean surface mixing, local air-sea interaction, coastal hydrodynamic characteristics, sediment movement, monsoon studies and ocean engineering.

In this study, wind and wave observational datasets were simultaneously collected in a nearshore area off Matara, Sri Lanka, which is the southernmost city of the Indian Peninsula and bordered by the northern Indian Ocean. The northern Indian Ocean is an important area for studying swells in the global wave climate, which persistently form in the southern oceans owing to the absence of land barriers (Alves, 2006). In addition, Sri Lanka is a good observation point for the southern Asian monsoon. Many wind and wave observations have been made in the Bay of Bengal (Glejin et al., 2013a; Nayak et al., 2013) and Arabian Sea (Aboobacker et al., 2011a; Glejin et al., 2013b); However, investigations of wind and waves in the waters south of

Sri Lanka, which hosts the busiest shipping lanes in the world, are scarce.

Although datasets from reanalysis projects (Semedo et al., 2010) and models (Sabique et al., 2012; Bhaskaran et al., 2014; Murty et al., 2014) are increasingly common, in situ observations (Rapizo et al., 2015) remain the most important reflections of the 'true' ocean and atmosphere state. Therefore, most major developments in the marine and atmospheric sciences have been closely related to the development of in situ observations.

The wind and wave dataset (Table 2) presented herein was collected from an automated weather station (AWS) and wave buoys to the south of Sri Lanka (see Figure 1 for location). The observation system, which began in 2011 and includes a 25 m meteorological tower and an acoustic sounder, is currently under construction. To date, a variety of marine atmospheric parameters have been measured, including temperature, air pressure, rainfall, wind, wave, and tide. Data from this observational system will be available for monsoon, air-sea interaction, and coastal dynamics research.

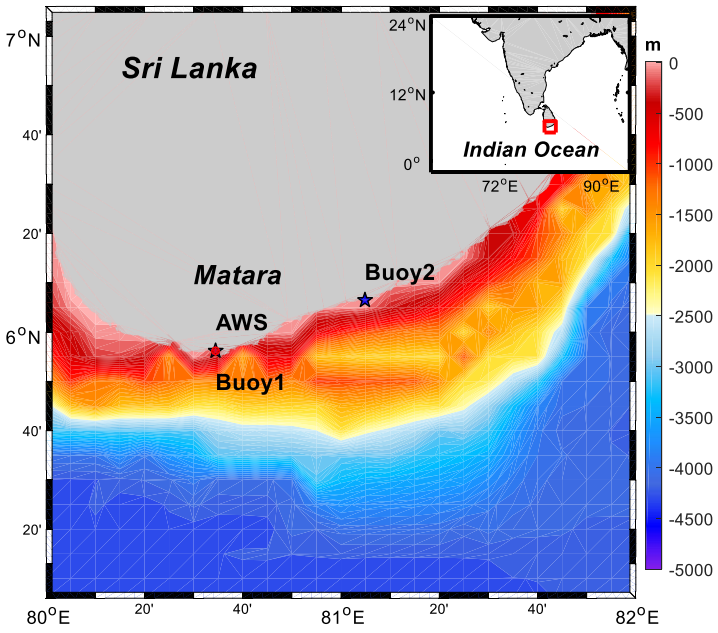

Figure 1 Observation deployment locations and topography (m).

2 Basic Data Description and Quality Control

The wind and wave dataset for Matara, Sri Lanka, consists of data obtained from three different observation instruments: AWS, Buoy 1, and Buoy 2. Table 2 shows the

details of the dataset and Figure 1 shows the locations of the instruments. After rigorous quality control, the time series of wind, air pressure, and surface waves from the AWS, Buoy 1, and Buoy 2 were used to generate datasets with temporal resolutions of 30 min, 10 min, and 1 h, respectively. At the data collection stage, 24 elements were measured in total. It was necessary to rigorously control data quality for all elements. The main technical processes involved in generating the dataset are shown as follows:

1) Calibration of all sensors

2) All data transferred in real-time to a storage facility (reduce or remove manual intervention)

3) Error detection

4) Deviation testing (remove records that deviate by > 3 standard deviations from the data mean)

To coincide with this publication, and in addition to the accompanying archived dataset spanning 2012–2016, unrestricted access is now available from a live online data repository located at http://www.sciencedb.cn/dataSet/handle/447. Contact details are provided to external organizations (to which the authors have no affiliation) to request additional wave spectra, tidal and wind parameters, or other elements of real-time observations after October 2016.

Table 2 List of datasets

Data name	Location	Deployment	Period	Frequency
AWS	5.936 N 80.575 E	AWS	Nov 2012–Jun 2014, Nov 2015 to Oct 2016	30 min
Buoy 1	5.934 N 80.574 E	Wave buoy	Sep 2013–Feb 2014	10 min
Buoy 2	6.106 N 81.080 E	Wave buoy	Apr 2013–Apr 2014	1 h

2.1 Data collection methods

The data collected in southern Sri Lanka were taken from an integrated

observation system that included Buoy 1, Buoy 2, and the AWS, including AWS1 and AWS2 (Figure 2).

Buoy 1 data include significant wave height (SWH, Hs), maximum wave height (Hmax), 1/10 wave height (H10), mean wave height (Havg) and corresponding wave period, hourly air pressure, and water level every 10 min at a water depth of 20 m.

Buoy 2 data include hourly SWH, peak wave period (Tp), mean wave direction (MWD), and direction spectra at 10 m water depth.

AWS1 data extend from Nov 2012 to Jun 2014 and include temperature (Temp), relative humidity (Relhumidity), air pressure (Pressure), and 1-min and 3-s averaged wind speeds at a frequency of 30 min. AWS2 data extend from Nov 2015 to Oct 2016 and include temperature (Airtemp), relative humidity (Relhumidity), air pressure, mean and maximum 1-min averaged wind speed and direction at a frequency of 30 min.

Buoy 1, which was anchored at the bottom of the sea at a depth of 20 m in Sep 2013, was operated normally and continuously to collect water level and wave data for about five months. Buoy 1 measured many types of no-directional wave parameters, as well as air pressure at the sea surface and water level. It was powered with a cable, and accepted wave information with a pressure sensor, which was developed at the South China Sea Institute of Oceanology. Pressure data were recorded continuously at a rate of 1 Hz over 5 min. The data for every 10 min are processed as one record. At the location of Buoy 1, a new buoy will be installed in the near future.

Buoy 2, which measured both wave and water level for one year from Apr 2013 to Apr 2014, consists of two instruments, a self-contained wave buoy at a depth of 10 m and a water level gauge. To measure the waves, the instrument was set to a frequency of 2 Hz with a sampling period of 15 min. In addition, 15-min sampling was carried out at 1-h intervals. For water level measurements, sample recording was done at 10-min intervals. Tide level was computed using the 10-min average of the pressure height data.

Figure 2 AWS1 (right) and AWS2 (left)

The seaside AWS (AWS1, Figure 2) was installed in Dec 2012 and can measure meteorological parameters, including wind speed and direction, air temperature, air humidity, and air pressure at an elevation of 12 m. In Dec 2015, the AWS was upgraded and was moved about 5 m, with all sensors installed at an elevation of 1.5 m (AWS2). The sampling frequency and parameters were based on AWS1, with the addition of a shortwave radiation sensor. AWS2 is still working and is planned to remain in operation always.

Since AWS1 and AWS2 collected wind speed at heights of 12 m and 1.5 m, respectively, wind speed from the buoy (W_z) was transformed into wind speed at 10 m elevation (W_{10}) using the Prandtl 1/7 law approximation (Streeter et al., 1998) with the equation:

$$W_{10}/W_z = (10/z)^{1/7}, \quad \text{Equation 1}$$

where z is the wind measurement height of the buoy.

2.2 Parameter descriptions

The dataset contains wind and wave data in Excel files. For Buoy 1, wave parameters were obtained directly using the zero-cross method. The main wave parameters for Buoy 2 were obtained by calculating the wave spectrum.

The H_s is given as

$$H_s = 4\sqrt{m_0},$$

$$T_m = \frac{m_0}{m_1} \qquad \text{Equation 2}$$

$$T_z = \sqrt{\frac{m_0}{m_2}},$$

where, m_n is the n^{th} moment of spectral density, and T_m and T_z are the mean wave period and zero-crossing wave period, respectively.

The energy-averaged mean wave direction (α_m) was determined as:

$$\alpha_m = \frac{1}{m_0}\int S(f)\alpha(f)df, \qquad \text{Equation 3}$$

where, $S(f)$ and $\alpha(f)$ are the directional distributions.

3 Verification of Reanalysis Wave Data

To study the impact on oceans from climate change, long-term datasets are needed; however, the lengths of continuous wave records are usually only a few to tens years. An important use of observational wave and wind data is model validation and assimilation. The ERA-Interim is based on the global atmospheric reanalysis product of the European Centre for Medium-Range Weather Forecasts (ECMWF) and is available from 1979 onwards (Dee et al. 2011). It comprises long-term and continuous grid data and is useful for wave extreme values, long-term variability of wave climate, and monsoon studies. Relative to the ERA-40 system, ERA-Interim incorporates many important IFS improvements, such as model resolution and physics changes, the use of four-dimensional variational (4D-Var) assimilation, and various other changes in the analysis methodology (Dee & Uppala, 2008, 2009). Furthermore, a reduction in the root-mean-square error of SWH against buoy data makes it smaller than that in ERA-40 (Bidlot et al., 2007). By comparison with observation data, the accuracy of ERA-Interim reanalysis data can be assessed, providing the basis to quantify monthly, inter-annual, and decadal variability of the wind and wave climate.

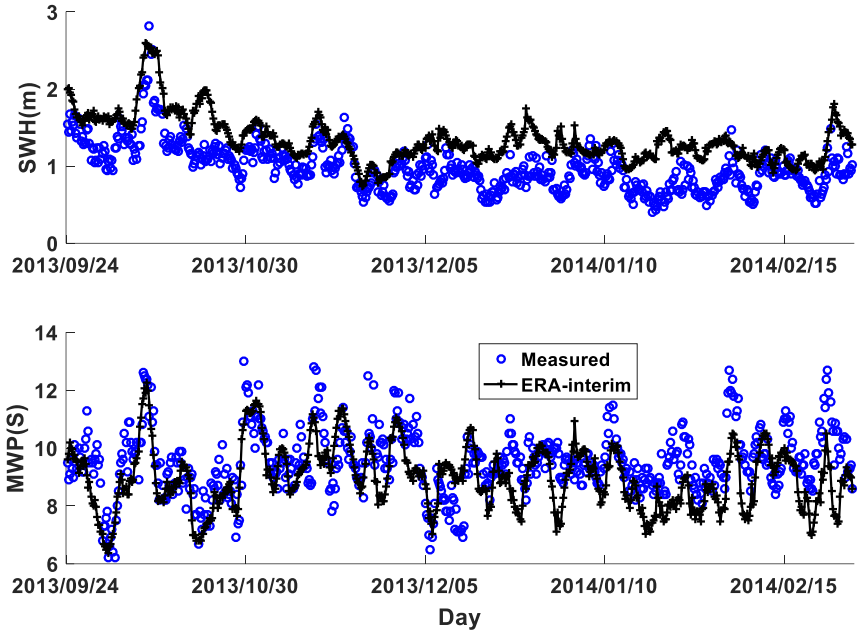

Figure 3 Time series of significant wave height (SWH) and mean wave period (MWD) for 24 Sep 2013–28 Feb 2014 (Buoy 1)

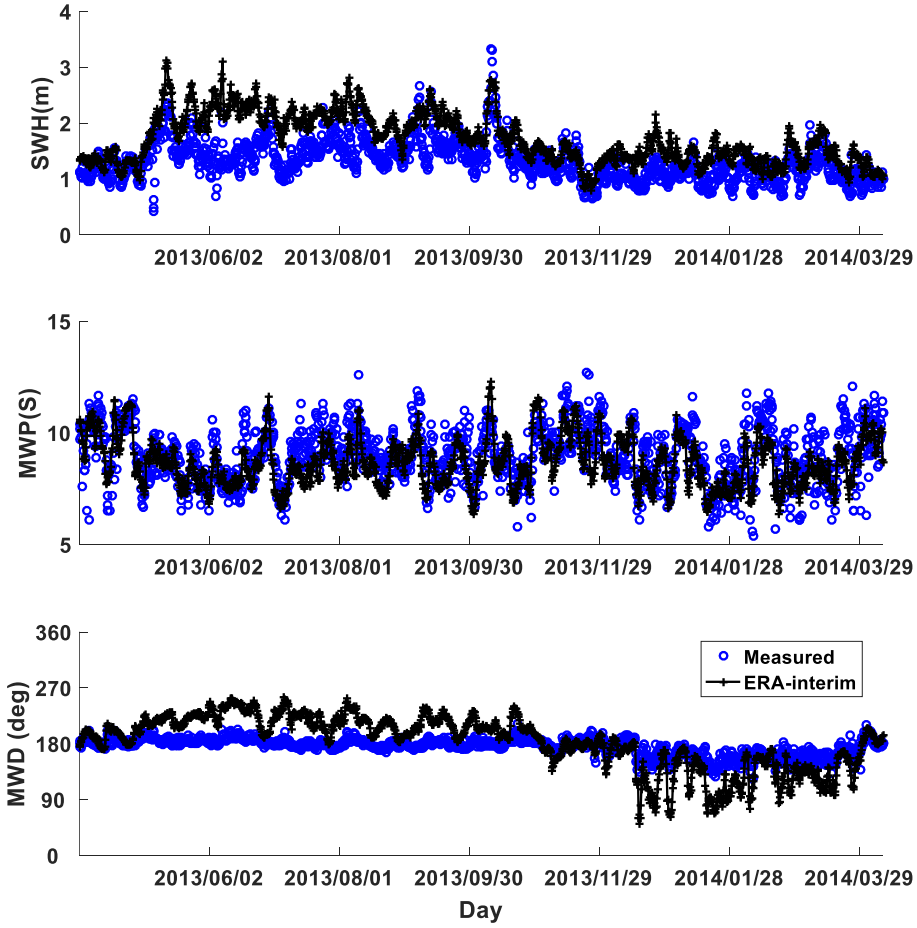

Figure 4 Time series of significant wave height (SWH), mean wave period (MWP), and mean wave direction (MWD) for 3 Apr 2013–9 Apr 2014 (Buoy 2)

Extensive inter-comparison and evaluation of wind stress estimates from the reanalysis data set (ERA-Interim) against available in situ observations have been performed for the tropical Indian Ocean (Praveen et al., 2013). The verification of SWH in the reanalysis data set has been done only for the Arabian Sea and Bay of Bengal (Shanas and Kumar, 2014a, b). In the present study, the nearest available ERA-Interim SWH data to the measured in situ buoy data from 2013 and 2014 were used for comparison. (Figure 3, Figure 4 and Figure 5). The comparison between the reanalysis and measured SWH data shows a general mean correlation (correlation coefficient = 0.747) with a general mean RMSE (0.435 m) during both years. For the MWP, the mean correlation coefficient and mean RMSE are 0.618 and 1.084; therefore, there are significant errors in the measurements, especially for MWD. These could be caused by the complicated near-shore geometry and/or by the resolution of the large-scale ERA-interim model, which is so low that it cannot describe changes in the complex seabed terrain.

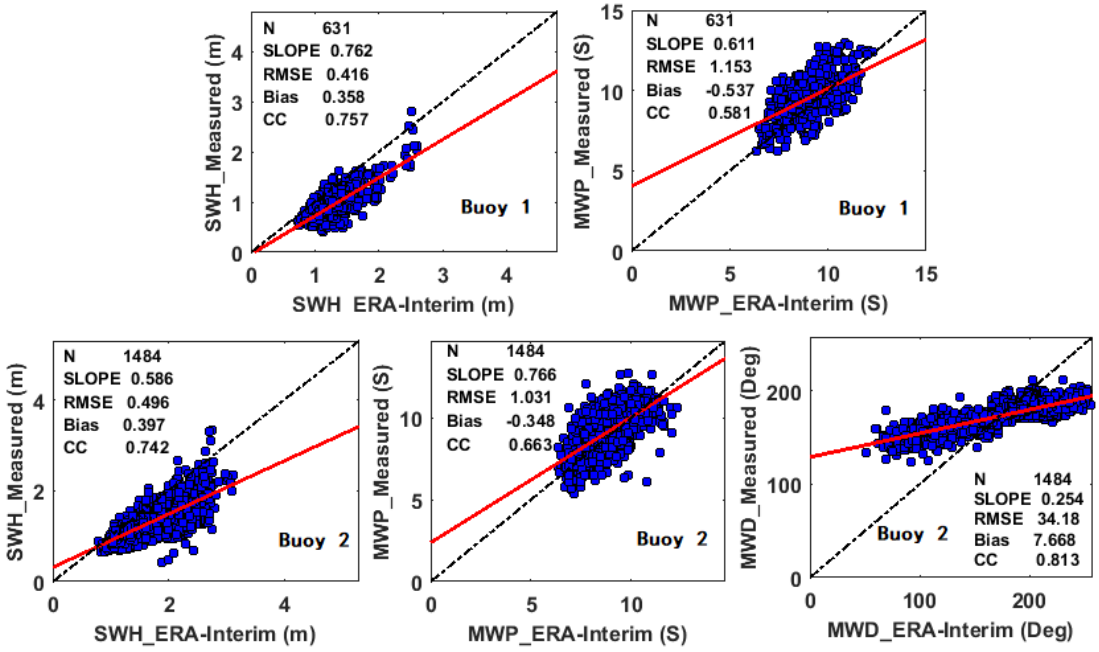

Figure 5 Scatter plots of SWH and mean wave period from the ERA-Interim. The displayed statistics include *N* = number of samples, *SLOPE* = slope of least-square regression, *RMSE* = root mean square error, *Bias* = bias, and *CC* = Pearson's correlation coefficient.

4. Wind Data Records

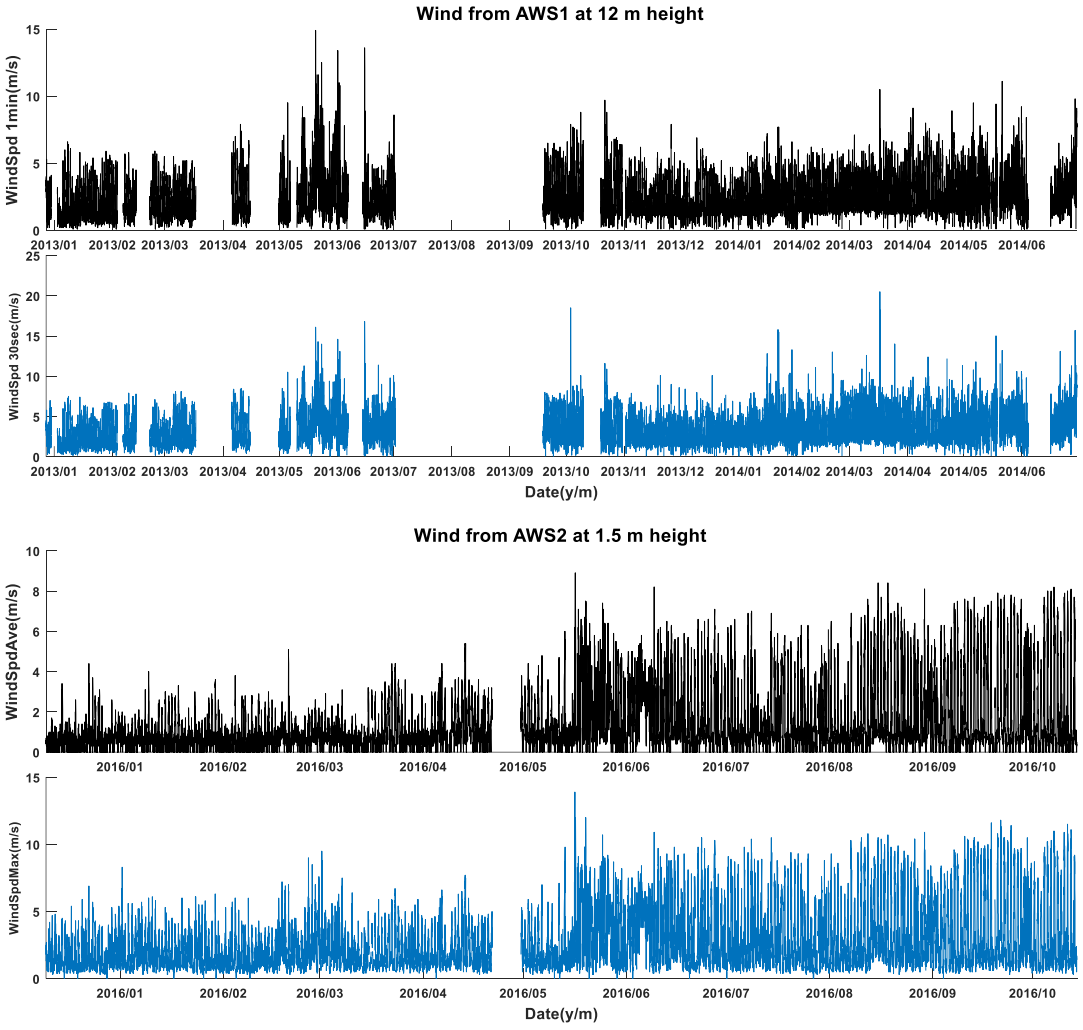

Figure 6 Measurements of wind speed

The wind is mainly controlled by NE and SW monsoon in the area. The wind speed and wind direction were measured at AWS1 and AWS2 (see Figure 6 for the time series of wind speed). The maximum measured wind was 8.9 m/s and the maximum gust 13.9 m/s. The wind sensors of AWS1 and AWS2 are at 12m and 1.5m height respectively. Due to in a high position, the coastal orography had no apparent impact on AWS1. But for AWS2, the wind speed was small during NE monsoon and was obviously effected by the landform of northern land (see Figure 1). During SW monsoon, the wind come from sea and the effect was weak for AWS2. This is why there was a significant lower wind speed during the winter months than the summer months, see Table 3. The monthly mean wind speed was the highest in September 2016 and lowest in December

2015 (Table 3).

Table 3 Monthly average values for averaged wind speed and maximum wind speed from AWS2.

(*WSA*: veraged wind speed, *WSM*: maximum wind speed, *num*: the number of effective data)

	WSA	WSA_{max}	WSM	WSM_{max}	num
	m/s	m/s	m/s	m/s	
201512	0.69	4.40	1.65	6.9	1067
201601	0.77	4.00	1.81	8.3	1488
201602	0.75	5.10	1.84	9	1383
201603	0.89	4.40	1.98	9.5	1447
201604	1.27	5.40	2.14	7.7	1011
201605	1.76	8.90	3.00	13.9	1456
201606	1.89	8.20	3.40	10.9	1435
201607	1.44	7.00	2.80	10.5	1470
201608	1.72	8.40	3.20	10.9	1484
201609	2.17	7.90	3.67	11.8	1418
201610	2.05	8.20	3.38	11.5	632

5. Wave Data Records

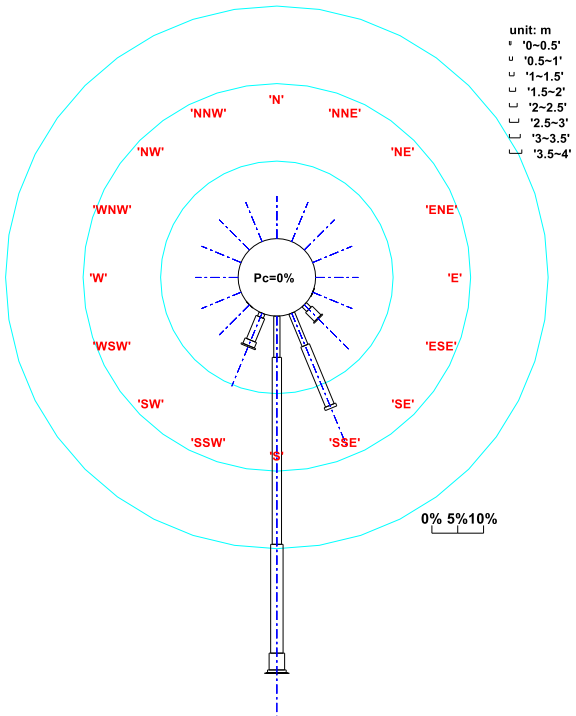

Figure 7 Wave rose of significant wave height for Buoy 2. South waves accounted for 69.12% of the total.

The integrated rate of wave data in Buoy 2 is high (96.38%); therefore, we investigated the characteristics of the wind sea and swell using the data from Buoy 2. The frequency range of the measured wave spectra was ~0.026–0.3 Hz. The frequency

associated with the peak energy is indicative of the dominant wave system over the region at that time. The wind sea and swell parameters were separated by frequency. Figure 8 show the time-series SWH, wind sea SWH, and swell SWH. Waves in the Indian Ocean vary in response to prevailing wind systems according to the month, and include inter-Monsoon-1 (IM1), southwest (SW) monsoon (May–September), inter-Monsoon-2 (IM2) (October–November), and northeast (NE) monsoon (December–February).

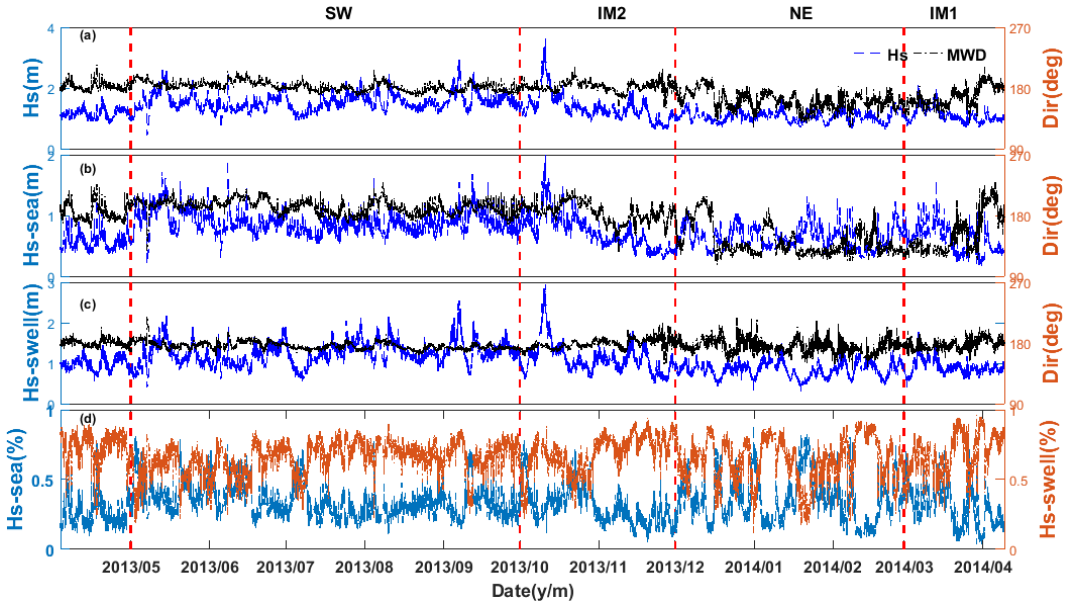

Figure 8 Time series of (a) SWH, (b) mean wave direction for SWH, (c) wind sea and swell, and (d) percentage dominance of wind sea and swell (Buoy 2).

Table 4 shows the monthly dominance of swell and wind sea on wave energy. Swells are predominant (> 50% in height) throughout the whole year. The maximum swell dominance is 77.6%, which occurs in November. The role of wind seas is significant in January and May (i.e., percentage dominance of wind seas is > 40%), and the maximum wind seas dominance is 42.4% and occurs in May. Annually, 66.1% of the waves are dominated by swells. Even though swells are predominant year-round, wind seas contribute sufficiently to the resultant waves during the SW (35.18%) and NE (36.7%) monsoon seasons. During the inter-monsoon periods, wind weakening and wind sea strengthening were reduced accordingly. Waves from the south accounted for 69.12% of all waves annually (Figure 7), mainly driven by swells, which predominate

throughout the year. As a result, the wave climate in this area is controlled mainly by long swells.

From Figure 8(b), the wind sea directions are southwest and northeast. In the NE monsoon period, the wind sea SWH is less than that during the SW monsoon period. Regarding swells, the wave direction throughout the year is predominantly south, although there are some small fluctuations after the SW monsoons. However, as with the wind sea, the SWH is bigger in the SW monsoon period. These phenomena originate from a mixture of the geographic location of Buoy 2 and prevailing wind systems. Buoy 2 is almost completely unsheltered from the south. In the SW monsoon season, except for long waves from the Southern Ocean, strong winds and sufficient fetch allow swells to grow and evolve in the northern Indian Ocean. However, because Buoy 2 is located nearshore with a short fetch, wind sea during the NE monsoon season is weaker. The NE monsoon has an inhibiting effect on swells from the south; therefore, there are small fluctuations in wave direction, and reductions in SWH during the NE monsoon season.

Table 4 Monthly percentage dominance of swell and sea.

Month	Swell (%)	Sea (%)
Jan	59.1	40.9
Feb	67.9	32.1
Mar	66.8	33.2
Apr	74.4	25.6
May	57.6	42.4
Jun	61.9	38.1
Jul	68.2	31.8
Aug	68.8	31.2
Sep	67.5	32.5
Oct	60.5	39.5
Nov	77.6	22.4
Dec	62.9	37.1

The unique geographic location of Sri Lanka, south of the Indian Peninsula, yields a different wave climate from those in the Bay of Bengal (Glejin et al., 2013) and Arabian Sea (Aboobacker et al., 2011), which are also located in the northern Indian Ocean and experience the same prevailing wind systems. Compared with the above two water bodies, the swells have a larger impact on wind sea.

Acknowledgments

We thank the China-Sri Lanka joint Center for Education and Research for providing hydro-meteorology observations. We also gratefully acknowledge the ECMWF Science Team for providing the ERA-Interim dataset. The work was supported by the International Partnership Program of the Chinese Academy of Sciences (grant no. 131551KYSB20160002).

Author Contributions

Y. L. and D.W. designed the study and wrote the manuscript. Y. L., F. Z., T. P. G., C. M. W. and T. L. performed the data collection, quality control, generation, and validation.

References

Aboobacker, V. M., Rashmi, R., Vethamony, P., & Menon, H. B. (2011a). On the dominance of pre-existing swells over wind seas along the west coast of india. *Continental Shelf Research, 31*(16), 1701–1712.

Aboobacker, V. M., Vethamony, P., & Rashmi, R. (2011b). "Shamal" swells in the Arabian Sea and their influence along the west coast of India. *Geophysical Research Letters, 38*(38), 1–7.

Alves, J. H. G. M. (2006). Numerical modeling of ocean swell contributions to the global wind-wave climate. *Ocean Modelling, 11*(1–2), 98–122.

Bhaskaran, P. K., Gayathri, R., Murty, P. L. N., Bonthu, S. R., & Sen, D. (2014). A numerical study of coastal inundation and its validation for thane, cyclone in the Bay of Bengal. *Coastal Engineering, 83*(1), 108–118.

Dee D. P. & Uppala S. M. (2008). 'Variational bias correction in ERA-Interim'. Technical Memorandum No. 575, ECMWF: Reading, UK (available from www.ecmwf.int/publications).

Dee, D. P. & Uppala, S. (2009). Variational bias correction of satellite radiance data in the era-interim reanalysis. *Quarterly Journal of the Royal Meteorological Society*, 135(644), 1830–1841.

Dee, D. P., Uppala, S. M., Simmons, A. J., Berrisford, P., Poli, P., & Kobayashi, S., et al. (2011). The era-interim reanalysis: configuration and performance of the data assimilation system. *Quarterly Journal of the Royal Meteorological Society*, 137(656), 553–597.

Murty, P. L. N., Sandhya, K. G., Bhaskaran, P. K., Jose, F., Gayathri, R., & Nair, T. M. B., et al. (2014).

A coupled hydrodynamic modeling system for phailin cyclone in the Bay of Bengal. *Coastal Engineering, 93*(93), 71–81.

Nayak, S., Bhaskaran, P. K., Venkatesan, R., & Dasgupta, S. (2013). Modulation of local wind-waves at Kalpakkam from remote forcing effects of southern ocean swells. *Ocean Engineering, 64*(6), 23–35.

Trageser, J. H. & Elwany, H., "The S4DW-an integrated solution to directional wave measurements," *Proceedings of the IEEE Fourth Working Conference on Current Measurement*, Clinton, MD, 1990, pp. 154-168. doi: 10.1109/CURM.1990.110902.

Glejin, J., Kumar, V. S., & Nair, T. M. B. (2013a). Monsoon and cyclone induced wave climate over the near shore waters off Puduchery, south western Bay of Bengal. *Ocean Engineering*, 72(4), 277–286.

Glejin J., Kumar, V. S., Nair, T. M. B., & Singh, J. (2013b). Influence of winds on temporally varying short and long period gravity waves in the near shore regions of the eastern Arabian Sea. *Ocean Sci*., 9, 343–353.

Rapizo, H., Babanin, A. V., Schulz, E., Hemer, M. A., & Durrant, T. H. (2015). Observation of wind-waves from a moored buoy in the southern ocean. *Ocean Dynamics, 65*(9), 1275–1288.

Shanas, P. R., & Sanil Kumar, V. (2014a). Temporal variations in the wind and wave climate at a location in the eastern Arabian Sea based on era-interim reanalysis data. *Natural Hazards & Earth System Sciences*, 14(5), 7239–7269.

Shanas, P. R., & Kumar, V. S. (2014b) Trends in surface wind speed and significant wave height as revealed by ERA-Interim wind wave hindcast in the Central Bay of Bengal, In*t. J. Climatol*., doi: 10.1002/joc.4164.

Sabique, L., Annapurnaiah, K., Nair, T. M. B., & Srinivas, K. (2012). Contribution of southern Indian Ocean swells on the wave heights in the northern Indian Ocean—a modeling study. *Ocean Engineering, 43*(2), 113–120.

Semedo, A., Sušelj, K., Rutgersson, A., & Sterl, A. (2010). A global view on the wind sea and swell climate and variability from ERA-40. *Journal of Climate, 24*(5), 1461–1479.

Streeter, V. L., Wylie, E. B., & Bedford, K. W. (1998). Fluid Mechanics. McGraw-Hill, Singapore.